Malaysian Journal of Medicine and Health Sciences (eISSN 2636-9346)

ORIGINAL ARTICLE

Metal Artefact Reduction with Different Transverse Angles of Metal Placement and Gantry Tilt Angulation in Spine CT Imaging

Noor Diyana Osman[1], Nurhidayah Mohamad Suhaimi[2], Halimatul Asma Saidun[1], Mohd Amir Syahmi Mat Razali[1,3], Nurul Fathin Mohd Sobri[1]

[1] Oncological and Radiological Sciences Cluster, Advanced Medical and Dental Institute, Universiti Sains Malaysia, Bertam, 13200 Kepala Batas, Penang, Malaysia
[2] Department of Radiotherapy and Oncology, Hospital Sultan Ismail, 81100 Johor Bahru, Johor Bahru, Johor, Malaysia
[3] Imaging Unit, Clinical Trial Complex, Advanced Medical and Dental Institute, Universiti Sains Malaysia, 13200 Kepala Batas, Malaysia

ABSTRACT

Introduction: Computed tomography (CT) has been widely used for postoperative spine assessment. However, the effectiveness of CT is limited by the presence of multiple artefacts surrounding metal implants. An artefact causes degradation of image quality and obscures the interpretation of spine CT images by a radiologist. The purpose of this study was to evaluate the optimum angle of gantry tilt and metal rod placement which produced the least metal artefact on CT images. **Methods:** A customised phantom was developed with different transverse angles of metal placement. The transverse angles of metal placement inside the phantom varied at 20°, 30°, 40° and 45°. The phantom was scanned with CT scanner at 0° axial scan angle. It was followed by acquisitions at different gantry tilt angles ranging from −12° to 20°. Quantitative and qualitative assessment by determining the signal-to-noise ratios (SNRs) of the CT images was performed. **Results:** The severity of the metal streak artefact increased as the metal insertion angles became wider up to 45° due to the widespread of streaking area. The severity of artefacts was reduced with the increment of the gantry tilt angle, which was observed in images acquired at 20°. **Conclusion:** For the gantry tilt angulation technique, the optimum gantry angle for metal artefact reduction is at the widest angle, which is +20° angulation. Although the gantry tilt technique did not eliminate the metal artefacts, it enabled a significant reduction of metal artefacts and improved image quality.

Keywords: Computed tomography; Gantry tilt angulation; Metal artefact; Postoperative spine imaging; Transverse angle

Corresponding Author:
Noor Diyana Osman, PhD
Email: noordiyana@usm.my
Tel: +604-5622421

INTRODUCTION

Pedicle screws are widely used for spinal fixation because they have been proven effective in stabilising spinal columns (1). An accurate postoperative evaluation by a radiologist is important to assess the positioning of spinal instrumentation and identify potential postoperative complications (2-4). Decisions on the choice of imaging technique for postoperative assessment depends on the type of spinal surgery, indications and materials used for the orthopaedic hardware (5-7). Each imaging modality has advantages and limitations for postoperative spine assessment. For example, radiography is the easiest and most inexpensive imaging technique. However, it is limited by overlaid structures in the two-dimensional image and does not portray the soft tissue details (8). Magnetic resonance imaging (MRI) is superior for diagnosing recurrent symptoms such as infection and lesion in soft tissues, but it is limited by magnetic susceptibility artefacts (9-11).

Among all modalities, computed tomography (CT) is the most reliable imaging technique and is currently the method of choice for postoperative spine evaluation. However, metallic spinal implants generate substantial artefacts on the CT images because of beam hardening, scatter effects and photon starvation (12-13). The metal artefact appears as dark and bright streaks protruding from the metal implants. The dark streak appearance is due to a beam-hardening effect and photon starvation that produce a dark signal when no photon is detected, and bright streaking is caused by the scattered photons as a low-frequency signal. The presence of multiple artefacts surrounding the metal implants causes degradation of image quality and may complicate the interpretation of spine imaging, thus affecting the diagnostic accuracy of soft tissue and bone pathology in patients. The severity of the metal artefacts increases with the atomic numbers (Z) of the implant material.

The artefacts are more pronounced with high Z metals such as iron or platinum and less pronounced with low Z metals such as titanium.

An important role of postoperative spine CT imaging is to identify mispositioning of pedicle screws. The accuracy of spinal screw placement into the pedicle is determined by a specific anatomy of the patient. One important anatomical parameter is the pedicle angle, which covers the angulation of the pedicle in both the sagittal (sagittal or cranial-caudal angle) and transverse (transverse or medio-lateral angle) planes. Fig. 1 shows the measurement of both pedicle angles, which is important for a safe pedicle screw placement procedure.

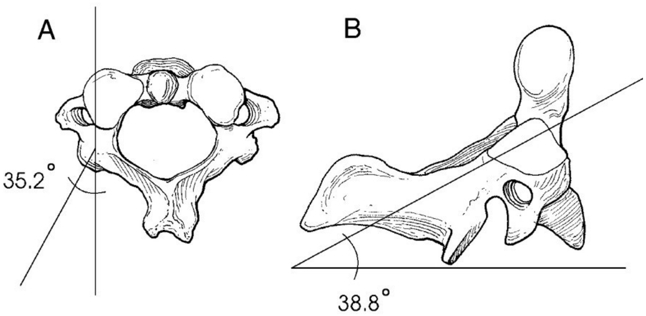

Figure 1: Two important angulations for pedicle screw placement: (A) the sagittal angle and (B) the transverse angle (adapted from [14]).

In this study, the degree of metal artefact was compared with different transverse angles of metal implant placement in the pedicle using a phantom study. The transverse angle was determined based on the pedicle's angle and the midline (medio-lateral angle). This medio-lateral inclination depended on the rotation of the vertebrae. For this study, the determination of the transverse angle for metal placement inside the phantom was performed through a retrospective survey of clinical images and a literature review. Previous literatures stated that the transverse pedicle angle of the vertebrae ranged from ±1.5° to 45° (1, 15-19).

This study also aimed to evaluate the reduction of metal artefacts using different gantry tilt angulations to determine the optimum tilting angle that would generate the least metal artefacts. Theoretically, a metal artefact was most apparent in the axial scanning plane. Gantry tilt angulation was one of the recommended techniques for the reduction of metal artefacts in CT imaging (12, 20). By tilting the gantry at a certain angle, the X-ray beam will transverse the metal at its smallest cross-sectional area, decreasing the beam attenuation and reducing the effect of the metal artefact in the CT image (8, 12). The tilted gantry technique changed the axial plane of the metal artefact outside of the axial slices of interest, and this allowed evaluation of structures adjacent to the metal object. Few studies have proven the effectiveness of gantry tilt angulation for the reduction of the artefact due to various metal implants such as dental fillings, knee prostheses and intracranial aneurysm clips (21-24).

MATERIALS AND METHODS

In this study, a customised water-bath phantom was used, similar to our previous works (25-26). The design of the phantom simulated the metal-induced artefacts due to pedicle screw fixation in postoperative assessment. The phantom was developed with materials having comparable attenuation properties to simulate human tissues. The phantom consisted of a Teflon rod with several holes for insertion of a metal rod to mimic the spine structure, as shown in Fig. 2(A). The phantom also included an acrylic rod that was placed opposite to the Teflon rod in the phantom to mimic soft tissue adjacent to the metal rod.

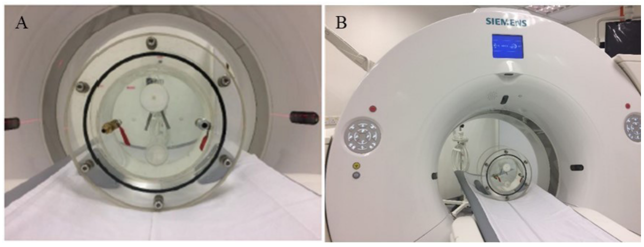

Figure 2: (A) The customised phantom used in phantom study and (B) The experimental setup for the phantom study with a customised water phantom with a stainless steel rod

The metal rod used in this study was made of stainless steel, which was the most commonly used material for spinal implants (Orthomedic Innovations Sdn Bhd, Penang, Malaysia). Modifications were made on the phantom at the Engineering Campus, Universiti Sains Malaysia (USM), Nibong Tebal, Malaysia. Two holes were drilled, and valves were implanted on the phantom lid to eliminate excessive water and air bubbles inside the phantom. The phantom study was performed with Siemens SOMATOM Definition AS+ CT Scanner (Siemens Healthcare, Germany) at the Imaging Unit, Advanced Medical and Dental Institute (AMDI), USM, Penang, Malaysia. The experimental setup is shown in Fig. 2(B). Phantom scanning was performed using the standard abdomen CT protocol with exposure settings of 120 kVp, 200 mAs and thin-slice thickness of 0.6 mm. Different acquisition kernels were used, including smooth (B30f) and sharp (B70f) kernels. The phantom was scanned using both helical and sequence acquisition modes. For the helical scanning mode, the lowest pitch value of 0.35 was used to obtain the overlapped scanning regions and to avoid missing data between the scanned areas. For the sequential mode, the number of scans was set at one and table feed was at 0 mm.

Transverse angle of metal insertion

The Teflon rods inside the customised phantom were drilled at different transverse angles for metal rod insertion. The size of the drilled hole for the insertion of the metal rod was 6 mm. The Teflon rod held a pair of stainless-steel rods with the actual length of a pedicle screw (6 cm). The transverse angles used in this study were based on the range of the transverse or medio-lateral angulation of normal human vertebrae. The determination of the transverse angles for metal placement inside the phantom was performed through retrospective review of images that was used to measure the range of transverse angles on clinical images and through literature review. Institutional committee review for the ethical approval of the clinical study was obtained (USM/JEPeM/16040156). Fig. 3 shows the range of transverse angles measured retrospectively on several selected clinical images.

The variations of the transverse angle for metal insertion studied were 20°, 30°, 40° and 45° from the midline of the Teflon rod, referring to the clinical images in Fig. 3. The Teflon rod was drilled with two holes for each transverse angle for insertion of a pair of stainless-steel metal rods. For each transverse angle, the placement of both metal rods was at the same transverse angulation and plane. The phantom was then filled with water to obtain a homogenous environment within the phantom background. The phantom was first scanned at 0° gantry angulation, followed by different gantry tilt angles (similar to previous studies), while maintaining the same acquisition parameters at the standard abdomen CT protocol.

Gantry tilting angulation

A tilted axial gantry technique was used by changing the angle of the scanning plane during data acquisition. Different gantry tilt angles (θ) were used: +20°, +16°, +12°, +8°, +4°, 0°, -4°, -8° and -12°. Zero degree of the scanning gantry meant that the gantry was not tilted. The positive values of the tilted angle referred to the gantry position that moved towards the patient table (antero-superior to postero-inferior), as shown in Fig. 2(B). The negative values of the tilted angle referred to the gantry position that moved away from the patient table (postero-superior to antero-inferior). The maximum angles of gantry tilting for this CT scanner were +20° and -12°.

Image quality analysis

Qualitative analysis was performed by visually comparing the degree of streaking on the reconstructed CT images by the radiologist and medical physicist. For quantitative evaluation, the mean CT number in Hounsfield unit (HU) and standard deviation (SD) were measured using regions-of-interest (ROIs) statistical analysis. Twelve ROIs were defined within the bright and dark streak regions (background with artefacts) adjacent to the metal rod on each CT image. The signal-to-noise ratio (SNR) was defined as in Equation 1:

$$\mathrm{SNR} = \frac{\text{Mean Signal}}{\text{Mean Noise (SD)}} \qquad \text{(Equation 1)}$$

Mean signal is the attenuation data which was expressed as the mean HU and noise was expressed as the standard deviation (SD) within the ROIs (27). The statistical analysis were performed on the SNR data using SPSS 2.0 software (IBM Corp, Armonk, New York, USA). T-test statistical analysis was performed to indicate the significant difference between mean SNR of tilted angles with non-tilted gantry.

RESULTS

Metal artefact reduction at different transverse angles of metal insertion

From the comparative study, the phantom images were better visualised with sharp kernels compared to smooth kernels. From the qualitative evaluation, sharp kernel images had a better spatial resolution and a better definition of a bony edge compared to smooth kernel images. Fig. 4 shows the appearance of metal

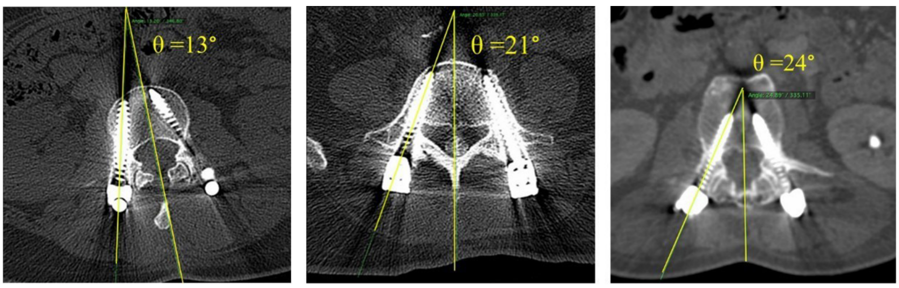

Figure 3: The transverse or medio-lateral angulation of pedicle screw placement measured on selected clinical images.

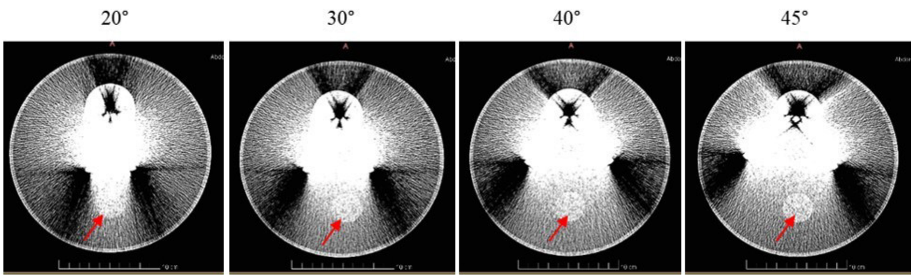

Figure 4: Severity of metal-induced artefacts with different transverse angles of metal placement in the range of 20° to 45°.

artefacts in CT images reconstructed with a sharp kernel (B70f) at different transverse angles of metal placement. However, sharp kernel images had higher noise, and thus produced lower SNR values compared to smooth kernels (B30f), as shown in Fig. 5. From Fig.5, it can be observed that, as the transverse angle of metal insertion increased, the severity of the streaking artefact for both bright and dark streaks also increased because of a wider area of metal-induced artefacts. The bright streak region became more significant with a wider insertion angle. However, the appearance of the acrylic rod that represented the soft tissue adjacent to the metal rods was better visualised in the phantom image with a wider transverse angle, at 45°, as shown by the red arrows in Fig. 4. Quantitative analysis was plotted as an SNR graph of the background region (with artefacts) adjacent to metal rods of different transverse angles at 0° of gantry angle. As can be observed from Fig. 5, the SNR showed a weak correlation with the transverse angle of metal placement for smooth kernel ($r = -0.43$) and strong correlation for sharp kernel ($r = 0.91$). The highest SNR was noted at a transverse angle of 40° for both smooth and sharp kernels.

Metal artefact reduction at different gantry tilt angulations

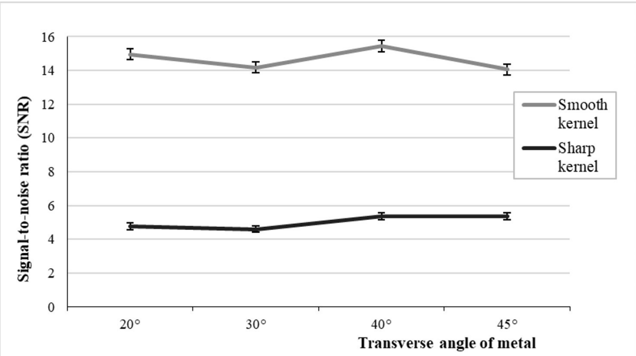

Figure 5: Graph showing the signal-to-noise ratio (SNR) in the background adjacent to metal rods at different transverse angles for both smooth and sharp kernel reconstructed images

Qualitative analysis was performed by comparing the most significant streaking image acquired at different gantry tilt angles for different metal insertion angles. Fig. 6 shows the streaking images for a metal insertion angle of 20°, acquired at different gantry tilt angles. The most severe streaking artefact was observed on the image acquired at 0° angle (no gantry tilt), and the image acquired at a gantry tilt angle of 20° showed the least artefacts. The appearance of the acrylic rod that represented the soft tissue adjacent to the metal rods was better visualised in a phantom image acquired with wider gantry tilt angles such as 20° and 16° (as marked by the red arrows in Fig. 6).

Quantitative analysis performed through ROIs statistical analysis of the background attenuation adjacent to a metal rod and the mean SNR value of the background were calculated in each image acquired at different gantry tilt angles. Fig. 7 shows a plotted graph of SNR values of the background region adjacent to metal rods in images acquired with different gantry tilt angles. From the comparative study of the SNR values between images acquired with smooth kernel (B20f) and sharp kernel (B70f), the results show that images of sharp kernel produce lower SNR values compared to those of smooth kernel, and the difference is statistically significant (p-value < 0.01).

There was no significant trend of SNR (p-value = 0.08) for sharp kernel, but it showed a significant difference (p-value = 0.04) of SNR for smooth kernel. For smooth kernel images, the highest SNR values were observed at a gantry tilt angle of 0° and the lowest SNR was at a gantry tilt angle of 20° (antero-superior to postero-inferior). Fig. 7 shows the SNR values plotted for each different transverse angle of metal rod placement and acquired at different gantry tilt angles. The highest SNR values were also observed at a gantry tilt angle of 0° and the lowest SNR was at a gantry tilt angle of 20° (antero-superior to postero-inferior) for all metal insertion angles.

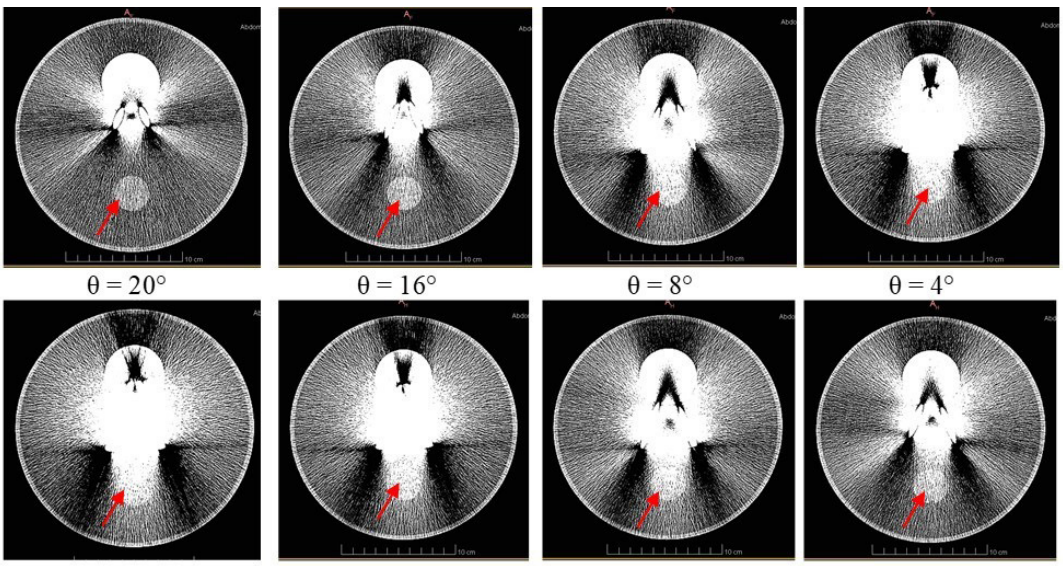

Figure 6: The figure illustrates the severity of the metal-induced artefacts in phantom images acquired with different gantry tilt angles (range of +20° to -12°) at metal insertion of 20°.

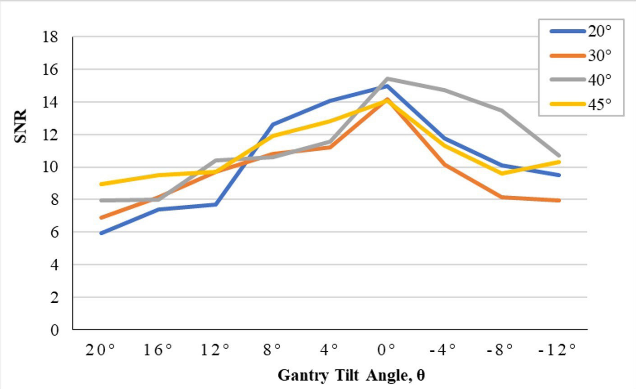

Figure 7: SNR values of the background region adjacent to metal rods in images acquired with different gantry tilt angulations and metal insertion angles

DISCUSSION

The transverse angles for metal placement in the spine are varied and specific to the anatomical structures of each individual. From the observation, it can be seen that the severity of both bright and dark streaking artefacts increases with a wider metal insertion angle (45°). The bright streak region became more significant with a wider insertion angle because of the widespread streaking area. However, the structure mimicking the soft tissue adjacent to the metal insert was clearly visualised at wider metal insertion angles. This is because, at a narrow metal insertion angle of 20°, visualisation of the soft tissue structure was impaired and overshadowed by bright streak artefacts that protrude from the neighbouring metal rod. As the angle became narrower, the concentration of artefacts was more at the centre of both metal rods. Moreover, the soft tissue structure also has a CT number like the bright streak background region. In real clinical evaluation, this can affect the diagnosis provided by a radiologist and lead to misdiagnosis.

Although the gantry tilt technique did not eliminate the metal artefacts, it enabled a significant reduction of metal artefacts and improved image quality. The severity of artefacts was reduced with the increment of the gantry tilt angle, which can be observed in the image acquired at 20°. Moreover, depiction of soft tissue-mimicking structures adjacent to the metal rods is also possible because of lesser streaking effects because of beam hardening and scatter. As mentioned earlier, by tilting the CT scanner gantry, the X-ray photon beam transverse the metal at its smallest cross-sectional area. Thus, the effects of the metal-induced artefact are reduced because of less interaction between the X-ray photons and the metal rods. The photoelectric absorption and scattered interaction were reduced as the area for interaction became smaller.

Bannas et al., (2012) showed that gantry tilt could reduce the metal artefact region, therefore improving the sensitivity of detecting oral tumours as tilted slices redistributed the metal artefacts to other locations outside of the slices where the tumour was located (21). Lewis et al., (2010) studied artefact reduction at 6 different tilt angles (±5°, 10°, and 15°) and reported that tilt angle of 5° to 10° was the optimal gantry angle to reduce the artefact in the adjacent tissues and angle of 15° for tibial component. Study done by Kim et al., (2018) also reported that additional tilted CT scan acquired at 15° suppressed the metal artefacts with their proposed MAR method. Both studies demonstrated that the artefact in the areas of interest was spread farther than the reconstructed slice acquired with direct axial at 0°, thus reducing the amount of artefact (23, 28). However, in our study, nine different angles were studied with the widest tilt angle of +20° and it resulted in optimal metal artefact reduction due to artefact displacement in axial slice. The wider the tilt angle will reduce the amount of artefact because the beam crosses the least amount of metal rod.

The highest value of mean SNR was observed at 0° tilt angle. As the gantry tilt angle increased in both directions, the value of mean SNR decreased. The lowest SNR was observed at a gantry tilt angle of 20° (antero-superior to postero-inferior). In this study, the high mean SNR value did not represent improvement in image quality because the SNR was calculated in the streaking ROIs. The high SNR in the streaking regions means a high degree of artefacts because of the high mean HU (signal) of the artefacts, which was observed at 0° tilt angle. The results also show that the SNR value in sharp kernel images is lower compared to smooth kernel. Sharp kernel allows a high-frequency signal and produces better edge definition, but the drawback of sharper kernel is that it causes high noise in CT images. The images will have a low mean value of SNR in return for a sharp detail of the image, but a smoother kernel generates images with lower noise but with poorer spatial resolution.

CONCLUSION

On the basis of the qualitative and quantitative analyses performed on the CT images, we can conclude that, as the transverse angle of metal insertion increases, the severity of the streaking artefact for both bright and dark streaks will also increase because of a wider area of metal artefact spread. For the gantry tilt angulation technique, we can conclude that the optimum gantry angle for metal artefact reduction is at the widest angle, which is +20° angulation. The tilted gantry approach may offer a solution of metal artefact problem in the evaluation of postoperative spine instrumentation with CT imaging.

ACKNOWLEDGEMENTS

This work was supported by Universiti Sains Malaysia (USM) under the Research University (RUI) Grant

[1001/CIPPT/811344]. We would also like to thank all staff at Imaging Unit, Clinical Trial Complex, AMDI USM, Penang, Malaysia and Department of Radiology, Hospital Universiti Sains Malaysia (HUSM), Kelantan, Malaysia for their help throughout the experiments.

REFERENCES

1. Gabitta A, Usman MM, Kishan A, et al. Pedicle screw placement in the thoracic and lumbar spine by the C-arm guided navigation and the free-hand method: A technical and outcome analysis. The J of Spinal Surgery 2016; 3 :90-5.
2. Hancock CR, Quencer RM, Falcone S. Challenges and pitfalls in postoperative spine imaging. Appl Radiol 2008; 37 :23-34.
3. Bittane RM, de Moura AB, Lien RJ. The postoperative spine: What the spine surgeon needs to know. Neuroimaging Clin 2014; 24 :295-303.
4. Dong Y, Shi AJ, Wu JL, et al. Metal artifact reduction using virtual monochromatic images for patients with pedicle screws implants on CT. Eur Spine J 2016; 25 :1754-63.
5. Thakkar RS, Malloy JP, Thakkar SC, et al. Imaging the postoperative spine. Radiologic Clinics 2012; 50 :731-47.
6. Ortiz AO. Postoperative Spine Imaging and Evaluation. Neuroimaging Clin 2014; 24 :xiii.
7. Herrera IH, de la Presa RM, Gutiйrrez RG, et al. Evaluation of the postoperative lumbar spine. Radiologнa (English Edition) 2013; 55 :12-23.
8. Douglas-Akinwande AC, Buckwalter KA, Rydberg J, et al. Multichannel CT: evaluating the spine in postoperative patients with orthopaedic hardware. RadioGraphics 2006; 26 :S97–110.
9. Hayashi D, Roemer FW, Mian A, et al. Imaging features of postoperative complications after spinal surgery and instrumentation. Am J Roentg 2012; 199: W123-9.
10. Ali AM. Evaluation of orthopedic metal artifact reduction application in three-dimensional computed tomography reconstruction of spinal instrumentation: a single Saudi center experience. J Clin Imaging Sci 2018; 8: 1-6.
11. Ross JS. Magnetic resonance imaging of the postoperative spine. Semin Musculoskel R 2000; 4 :0281-92.
12. Barrett JF, Keat N. Artifacts in CT: recognition and avoidance. RadioGraphics 2004; 24: 1679-91.
13. Boas FE, Fleischmann D. Evaluation of two iterative techniques for reducing metal artefacts in computed tomography. Radiology 2011; 259 :894-902.
14. Howington JU, Kruse JJ, Awasthi D. Surgical anatomy of the C-2 pedicle. J Neurosurg Spine 2001; 95 :88-92.
15. Panjabi MM, Goel V, Oxland T, et al. Human lumbar vertebrae. Quantitative three-dimensional anatomy. Spine 1992; 17 :299–306.
16. Benzel EC. Biomechanics of Spine Stabilization: Principles and clinical practices. McGraw-Hill, Health Professions Division; 1995.
17. Tan SH, Teo EC, Chua HC. Quantitative three-dimensional anatomy of cervical, thoracic and lumbar vertebrae of Chinese Singaporeans. Eur Spine J 2004; 13 :137-46.
18. Singh R, Srivastva SK, Prasath CS, et al. Morphometric measurements of cadaveric thoracic spine in Indian population and its clinical applications. Asian Spine J 2011; 5 :20–34.
19. Mattei TA, Meneses MS, Milano JB, et al. “Free-hand” technique for thoracolumbar pedicle screw instrumentation: Critical appraisal of current “State-of-Art”. Neurology India 2009; 57 :715-21.
20. Boas FE, Fleischmann D. CT artifacts: causes and reduction techniques. Imaging Med. 2012; 4 :229–40.
21. Bannas P, Habermann CR, Jung C, et al. Diagnostic accuracy of state-of-the-art MDCT scanners without gantry tilt in patients with oral and oropharyngeal cancer. Eur J Radiol. 2012; 81 :3947–52.
22. Lee, C, Evaluation of using CT gantry tilt scan on head and neck cancer patients with dental structure: scans show less metal artifacts. Radiological Society of North America 2011 Scientific Assembly and Annual Meeting, November 26–2 December 2011, Chicago IL. http://archive.rsna.org/2011/11030354.html (7 August 2018, date last accessed)
23. Lewis M, Toms AP, Reid K, et al. CT metal artefact reduction of total knee prostheses using angled gantry multiplanar reformation. Knee 2010; 17: 279–82.
24. Brown JH, Lustrin ES, Lev MH, et al. Reduction of aneurysm clip artifacts on CT angiograms: a technical note. AJNR Am J Neuroradiol 1999; 20: 694–6.
25. Osman ND, Salikin MS, Saripan MI. Metal streak analysis with different acquisition setting in postoperative spine imaging: A phantom study. World Acad of Sci and Tech. 2007; 35: 96-100.
26. Osman ND, Salikin MS, Saripan MI, et al. Metal artefact correction algorithm based-on DSAT technique for CT images. In Biomedical Engineering and Sciences (IECBES), 2014 IEEE Conference on 2014 Dec 8 (pp. 324-327). IEEE.
27. Paul J, Krauss B, Banckwitz R, et al. Relationships of clinical protocols and reconstruction kernels with image quality and radiation dose in a 128-slice CT scanner: study with an anthropomorphic and water phantom. Eur J Radiol 2012; 81 :e699-703.
28. Kim C, Pua R, Lee CH, Choi DI, Cho B, Lee SW, Cho S, Kwak J. An additional tilted-scan-based CT metal-artifact-reduction method for radiation therapy planning. Journal of Applied Clinical Medical Physics. 2019; 20(1): 237-49